Electronic Supplementary Material (ESI) for Journal of Materials Chemistry A.

Constructing Semiconductive Crystalline Nano-Porous Material By Coulomb Interactions

Guan-E Wang, Ming-Shui Yao, Min-Lan Cai, Jing-Wei Xiu, Yan-Zhou Li, Gang Xu*, Guo-Cong Guo*

State Key Laboratory of Structural Chemistry, Fujian Institute of Research on the Structure of Matter, Chinese Academy of Sciences, Fuzhou, Fujian 350002, P. R. China

Experimental section:

1. Materials

PbI_2, azobenzene (AZO), $CuCl_2 \cdot 2H_2O$, 2,2'-Bipyridine, *N*, *N*'-dimethyl formamide (DMF) HI, and ethanol were received from Sinopharm Chemical Reagent Co. Ltd. They were directly used without further purification.

2. Measurements.

PXRD patterns were collected on a MiniFlex II diffractometer using Cu-K_α radiation (λ = 1.540598 Å) at 30 kV and 15 mA. The simulated pattern of $(organic)_n(Pb_2I_6)_n$ (organic = $[Cu(2,2'\text{-bipy})_2I]^+$ for **1** and $[(H_2EDAB)^{2+}]$ for **2**; 2,2'-bipy = 2,2'-Bipyridine, $[(H_2EDAB)^{2+}]$ = $Et_2HNC_6H_4C_6H_4NHEt_2$) were derived from the Mercury Version 1.4 software. The FT-IR spectra were obtained on a VERTEX 70 FT-IR spectrometer using KBr disks in the range of 4000–400 cm^{-1}. The analyses of carbon, nitrogen and hydrogen contents were performed on an Elementar Vario MICRO microanalyser. A NETZSCH STA 449C thermogravimetric analyzer was used to obtain thermogravimetry (TG) curves in N_2 with a flow rate of 20 mL min^{-1} and a ramp rate of 10 °C min^{-1} in the temperature range of 30–800 °C. An empty Al_2O_3 crucible was used as the reference. Optical diffuse reflectance spectra were measured on a PerkinElmer Lambda-950 UV/Vis/NIR spectrophotometer. A $BaSO_4$ plate was used as a reference for sample measurements. Each sample was ground into fine powder and then

coated on a $BaSO_4$ wafer in a thin glass slide holder. The ESI-MS spectrum was measured by ThermoFinnigan DECAX-30000 LCQ Deca XP ion trap mass spectrometry. The crystal photographs at different direction were took from Super Nova CCD Diffractometer with the video camera towards the crystal direction. The single crystal electrodes were made using silver plastic for **1** and gold plastic for **2**, and 50 μm gold wire by placing the crystal between two electrodes. The temperature-dependent I-V curves were measured by KEITHLEY4200-SCS. Before carrying out adsorption experiments, the crystals of **2** (100 mg) were immerged in CH_3OH for three days, then degassed automatically in Micromeritics ASAP 2020-M at 60ºC for 24 h to generate the activated crystals of **2** for N_2, Ar and CO_2 absorption. Ethanol and methanol and water adsorption measurements were performed in the Intelligent Gravimetric Sorption Analyser IGA100B System at 25 ºC.

3. X-ray crystallographic study

The X-ray diffraction measurement was performed on a Rigaku Ultrax-Saturn 70 diffractometer using graphite monochromated Mo-K_α radiation (λ = 0.71073 Å). Intensity data set was collected using an ω scan technique and corrected for *Lp* effects. The primitive structure was solved by the direct method using the Siemens SHELXTL^{TM} Version 5 package of crystallographic software. The difference Fourier maps based on these atomic positions yield the other non-hydrogen atoms. The final structure was refined using a full-matrix least-squares refinement on F^2. All non-hydrogen atoms were refined anisotropically. Hydrogen atoms on carbon and nitrogen atoms were generated geometrically. Crystallographic data have been deposited with the Cambridge Crystallographic Data Centre: CCDC 917236. This datum can be obtained free of charge from The Cambridge Crystallographic Data Center via www.ccdc.cam.ac.uk/data_request/cif.

4. Synthesis of crystalline $[Cu(2,2'\text{-Bipy})_2I]_{2n}(Pb_2I_6)\cdot n DMF\cdot n H_2O$ (1: 2,2'-Bipy = 2,2'-Bipyridine)

A mixture of PbI_2 (0.116 g, 0.125 mmol), $CuCl_2\cdot 2H_2O$ (0.045 g, 0.125mmol), 2,2'-Bipy

(0.079 g, 0.25 mmol), DMF (3 mL), and concentrated HI (1.5 mL, 45%) was heated at 150 °C for 2 days in a sealed 25-mL Teflon-lined stainless steel vessel. Upon cooling at 2.5 °C·h^{-1} to room temperature, dark green sheet crystals of **1** were obtained in 95% yield (based on PbI_2). Elem. Anal. (%) Calcd.: C:23.35, H: 2.12, N: 5.92;. Found: C: 23.24; H: 2.07; N: 5.86.

5. Synthesis of crystalline $(H_2EDAB)_n(Pb_2I_6)_n$ (2: $H_2EDAB = Et_2NHC_{12}H_8NHEt_2$)

A mixture of PbI_2 (0.231 g, 0.5 mmol), AZO (0.046 g, 0.25 mmol), ethanol (3 mL) and concentrated HI (2 mL, 45%) was heated at 180 °C for 1.5 days in a sealed 25-mL Teflon-lined stainless steel vessel. Upon cooling at 5 °C·h^{-1} to room temperature, yellow prismatical crystals of **2** were obtained in 95% yield (based on PbI_2). Elem. Anal. (%) Calcd.: Cal. C: 16.28; H: 2.04; N: 1.90. Found: C: 16.31; H: 1.93, N: 1.96. $(H_2EDAB)^{2+}$ in compound **2** was generated through the *in situ* reaction among azobenzene, ethonal and HI (Table S2), which was confirmed by LC-ESI-MS^n spectrum (Figure S10) and IR spectroscopy (Figure S11). The purity of mechanically separated crystals were checked by powder X-ray diffraction (PXRD, Figure S12).

Traditional organic synthesis from AZO to H_2EDAB normally takes four steps in different reaction conditions (Scheme S1): 1) Hydrazobenzene from azobenzene under hydrogen high-pressure and alkaline conditions; 2) Rearrangement of hydrazobenzene to benzidine by acid catalysis; 3) *N*-alkylated products from the reaction of benzidine and alkyl iodides under alkaline conditions; Usually, alkyl iodides are obtained from alcohols activated by HI. Compared with these traditional multiple acidic and alkaline conditions, we only use one solvothermal condition, which makes the synthetic step simple and effective. The existence of H_2EDAB species in **2** has been proved by ESI-MS spectra (Figure S10). It is worth to note that the reaction cannot happen without PbI_2 and ethanol. Although the mechanism has yet to be investigated in detail, the present result is the first example of a clear transformation from AZO to H_2EDAB through one solvothermal step. The solvothermal technique accompanying the *in situ* syntheses of organic species can provide a more convenient and effective route for the novel inorganic–organic hybrids than with traditional methods.

6. Density of states (DOS)

Optical measurements confirm that compound **1** has absorption edge at 0.97 and 2.25 eV, while compound **2** has that at 2.73 eV (Figure S7a), respectively. To understand better the composition of electron transition barrier in $[(Pb_2I_6)^{2-}]_\infty$ chains, the two compounds were theoretically calculated by evaluation of the density of states (DOS), which were performed with the CASTEP code based on density functional theory using a plane-wave expansion of the wave functions. The isolated organic cations have little contribution to the electron transport in both compounds. the conductivity mainly originates from the electron transfer in $[(Pb_2I_6)^{2-}]_\infty$ chains. The partial DOS for **1** and **2** are illustrated in Figures S7b and S8: in **1**, the absorption edge of 0.97 eV is ascribed to the electron transition from I in $[Cu(2,2'\text{-Bipy})_2I]^+$ to Cu (Figure S8), and the absorption edge of 2.25 eV is ascribed to the electron transition from I to Pb in $[(Pb_2I_6)^{2-}]_\infty$ chain; in **2**, the absorption edge of 2.73 eV is ascribed to the electron transition from I to Pb (Figure S7b). The conductivity of **1** is similar to that of **2**, which is consistent with the similar electron transition barrier of $[(Pb_2I_6)^{2-}]$ chain in **1** with that in **2**.

7. Alcohol detection measurement

Two-terminal-probe direct current method was used for the sensor measurements of the single crystals of **2**. The sensor characterization was conducted by our previous reported instrument.[1] The methanol and ethanol vapor were generated by bubbling method and ethanol, repectively. It takes ~1.30 min to fulfil the quartz chamber when the gas flow was 600 ml min^{-1}. The constant flow was 600 ml min^{-1}. The bias on the device was 5 V and the current was recorded using Keithley 2602B Sourcemeter. The response of the device (R) can be explained by using the following equation[2]

$$G = (\sigma_{gas}-\sigma_{air})/\sigma_{air} = R_{air}/R_{gas} - 1 = A_g p_g^{\beta} \quad (1)$$

where σ_{air} denotes the conductance in the absence of the target gas, p_g is the gas partial pressure, A_g is a prefactor, and the exponent β is the response order.

Since the response is defined as $R_{air} / R_{gas} - 1$, eq. 1 can be rewritten as

$$\log R = \log(R_{air}/R_{gas} - 1) = \log A_g + \beta \log p_g \quad (2)$$

The detection limit for methanol and ethanol can be obtained by setting R = 0.1, respectively.

Supporting graphics:

Table S1. Shortest distances among the charge centers of cations and $[(Pb_2I_6)^{2-}]_\infty$ anion in **1** and **2**.

1		**2**	
Cu1···I1	8.239(3) Å	N1···I1	4.417(13) Å
Cu1···I2	5.923(2) Å	N1···I2	5.014(11) Å
Cu1···I3	5.787(2) Å	N1···I3	7.979(11) Å

Table S2. Crystallographic data for **2**.

Empirical formula	$C_{20}H_{30}N_2Pb_2I_6$
	2
Crystal Size (mm^3)	0.18×0.05×0.05
T (K)	293(2)
λ□ (Mo K_α, Å)	0.71073
Space group	P-4/2$_1c$
a (Å)	22.156(8)
b (Å)	22.156(8)
c (Å)	8.111(4)
β (°)	90
V (Å^3)	3982(3)
Z	8
D_{calcd} (g/cm^3)	2.459
μ (mm^{-1})	13.107
F(000)	2584
θ_{range} (°)	2.91 to 25.50
Indep. Reflns/R_{int}	3699/0.0801
Obs. Reflns.	2306 (I > 2sigma(I))
Final R indices (obs.)	$R1$ = 0.0637, $wR2$ = 0.1507
R indices (all)	$R1$ = 0.1135, $wR2$ = 0.1769
GOF on F^2	1.026
$\Delta\rho_{max}/\Delta\rho_{min}$ (e/Å^3)	1.292/–1.172

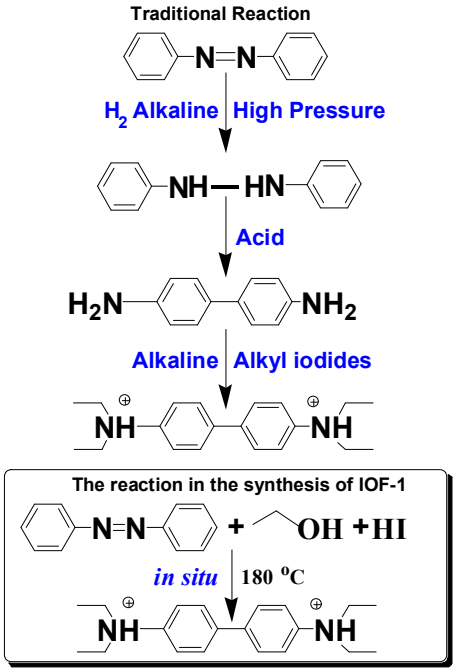

Scheme S1. Four reaction steps in the traditional synthesis process of **2**.

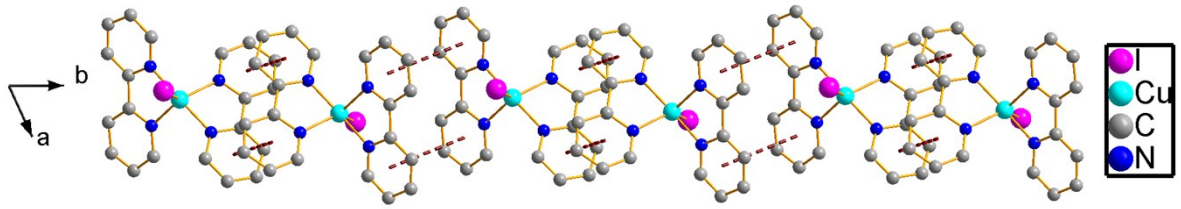

Figure S1. Face-to-face π···π interactions of Cu(2,2'-Bipy)$_2$I$^+$ cations in 1-D [Cu(2,2'-Bipy)$_2$I]$^+$ supramolecular chain with hydrogen atoms being omitted for clarity.

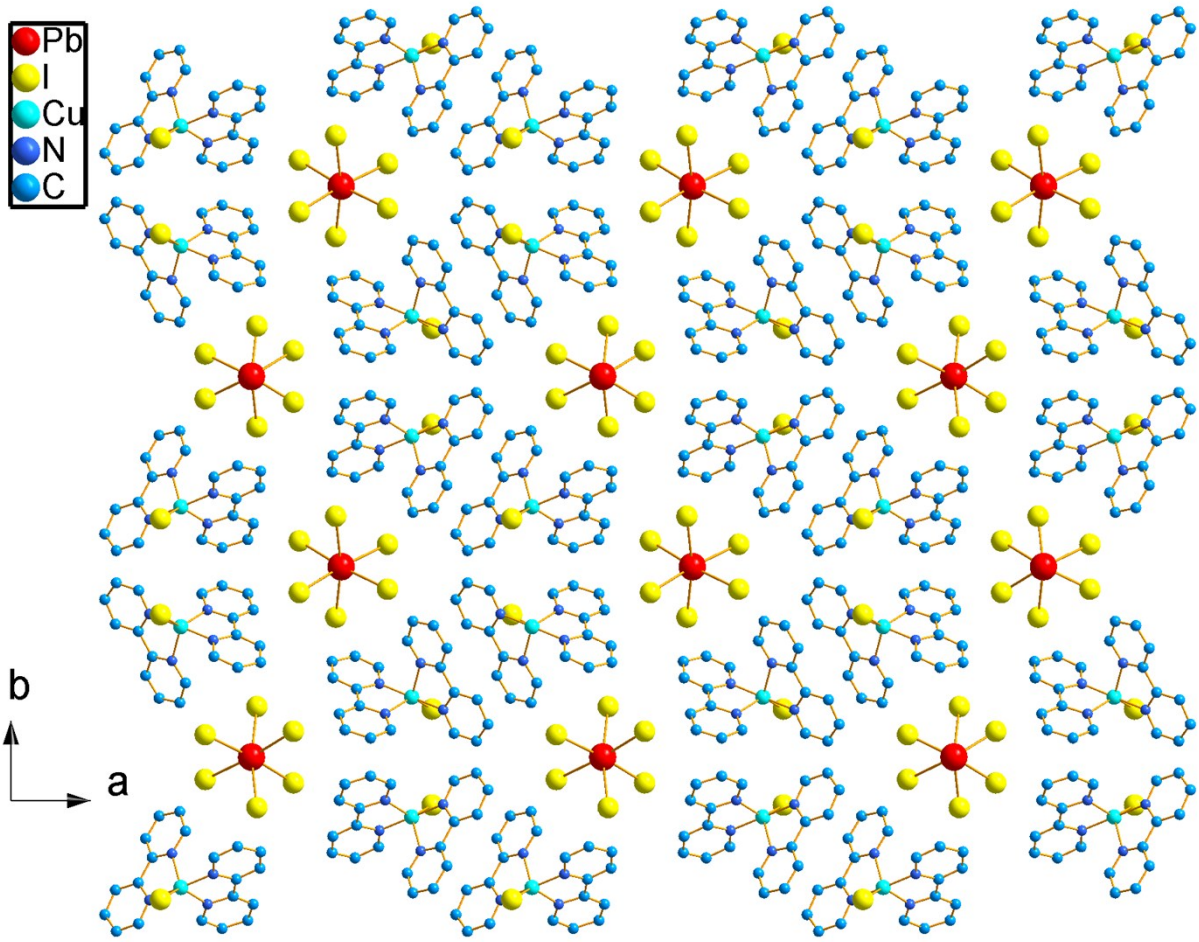

Figure S2. Close packing structure of compound **1** after heating to 100 ^{o}C for 2 hours.

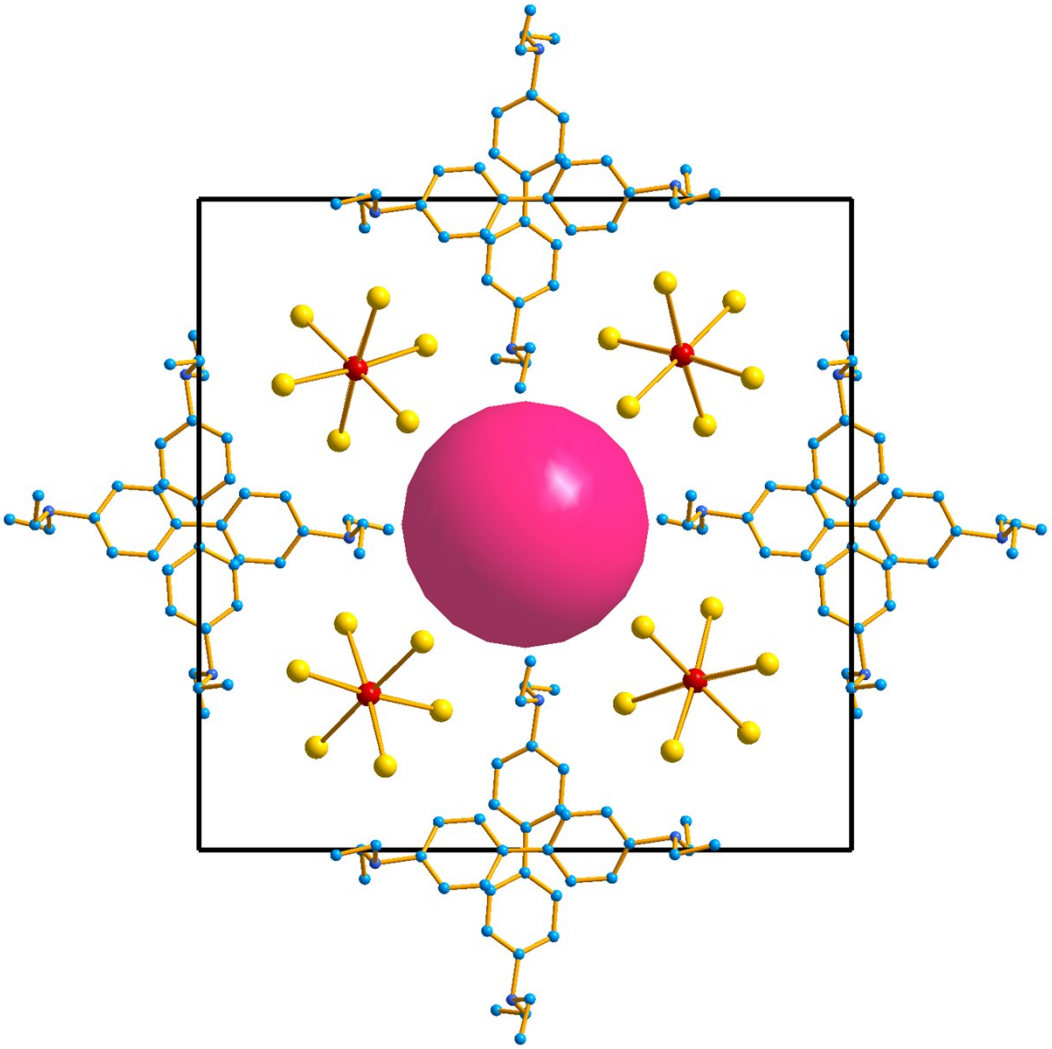

Figure S3. Microporous structure of 1-D channel (pink) in **2**, hydrogen atoms have been omitted for clarity.

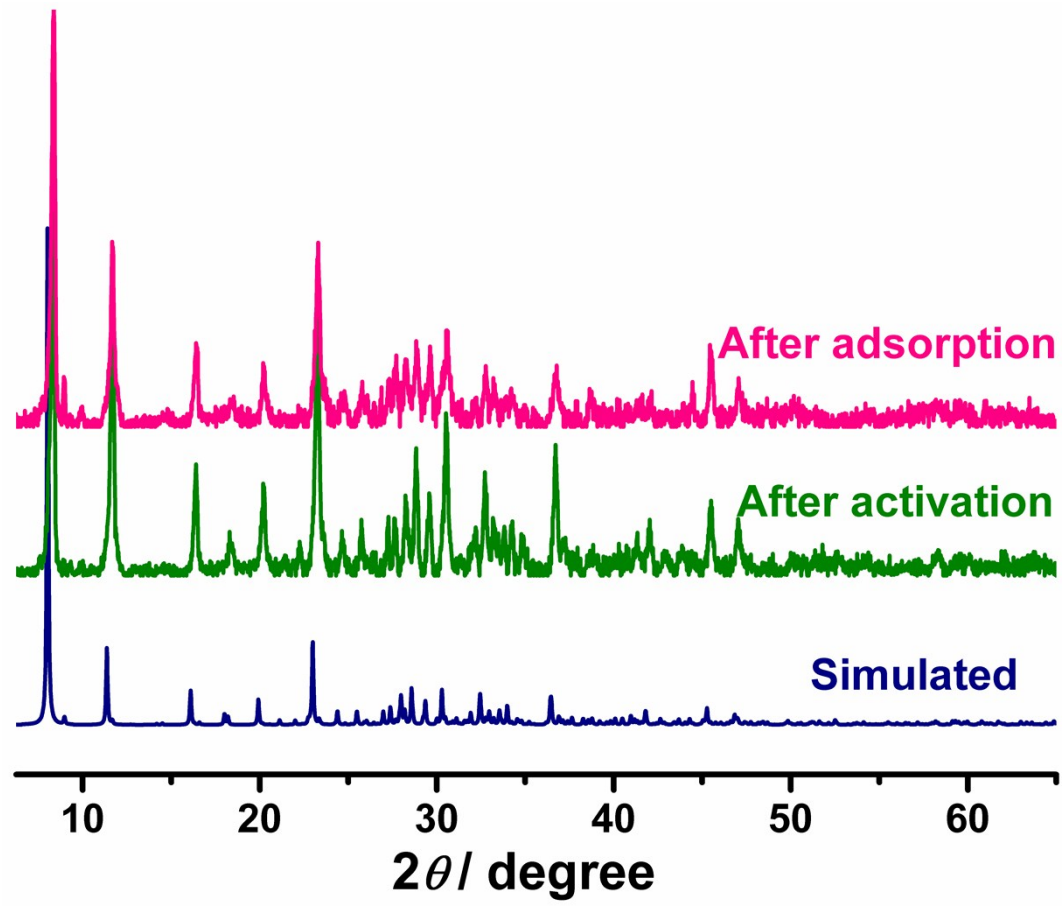

Figure S4. PXRD patterns for **2** after activation and adsorption measurements.

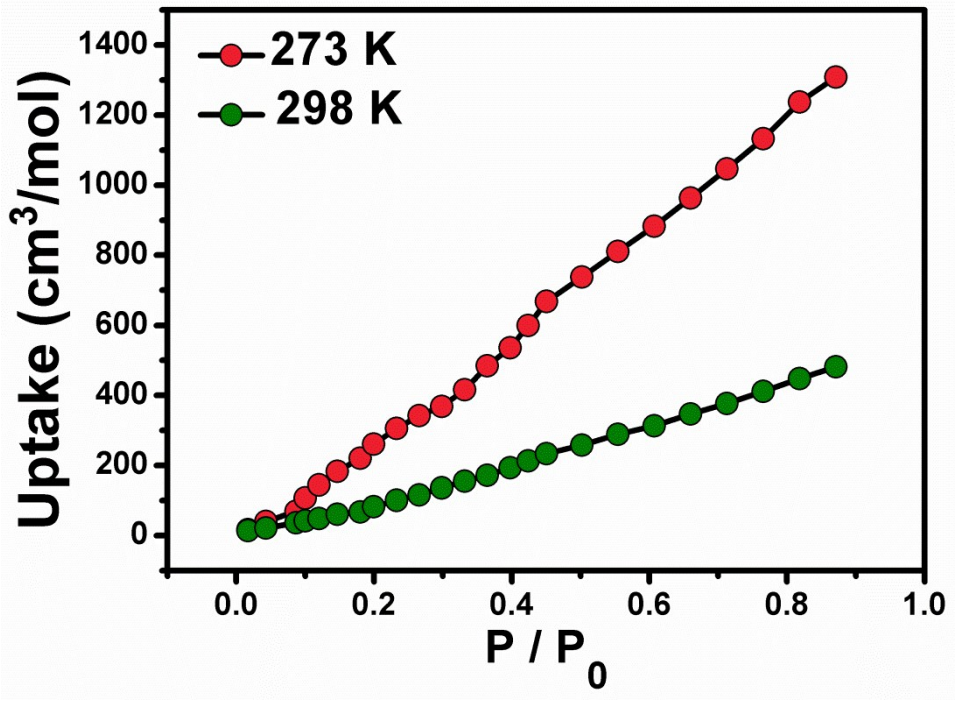

Figure S5. CO_2 adsorption isotherms for **2** at 273 and 298 K.

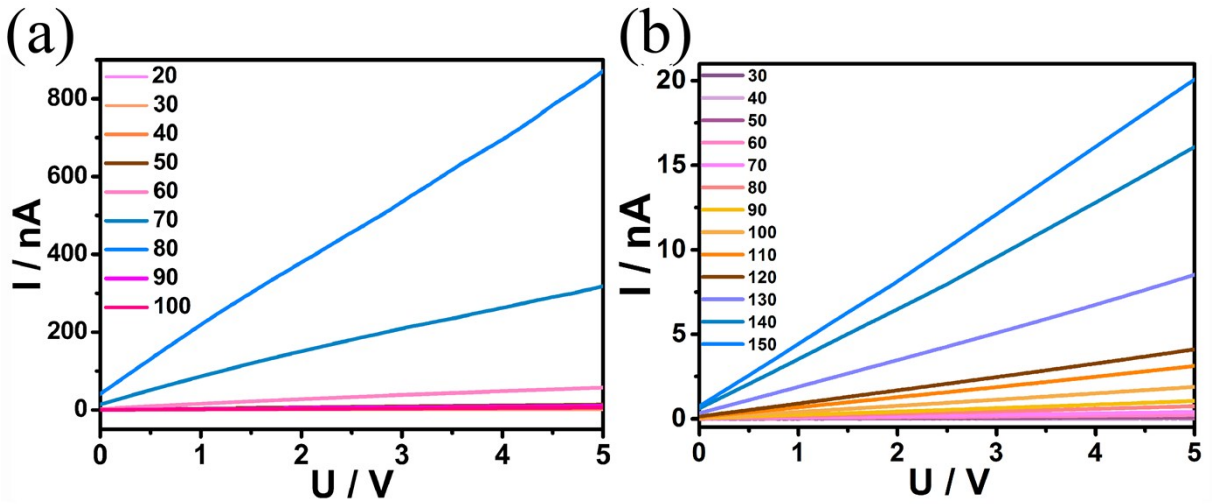

Figure S6. Temperature-dependent I-V curve for single crystal of **1** (a) and **2** (b) along *c* axis.

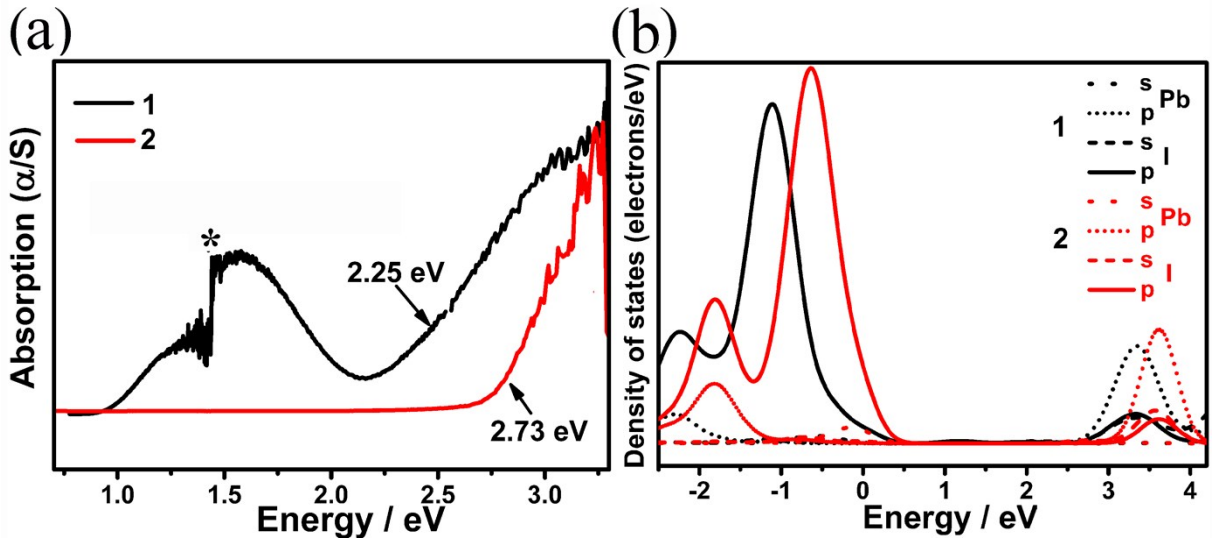

Figure S7. UV-Vis absorption spectra of **1** and **2** (a). Partial DOS for **1** and **2** (b). * is monochromator change.

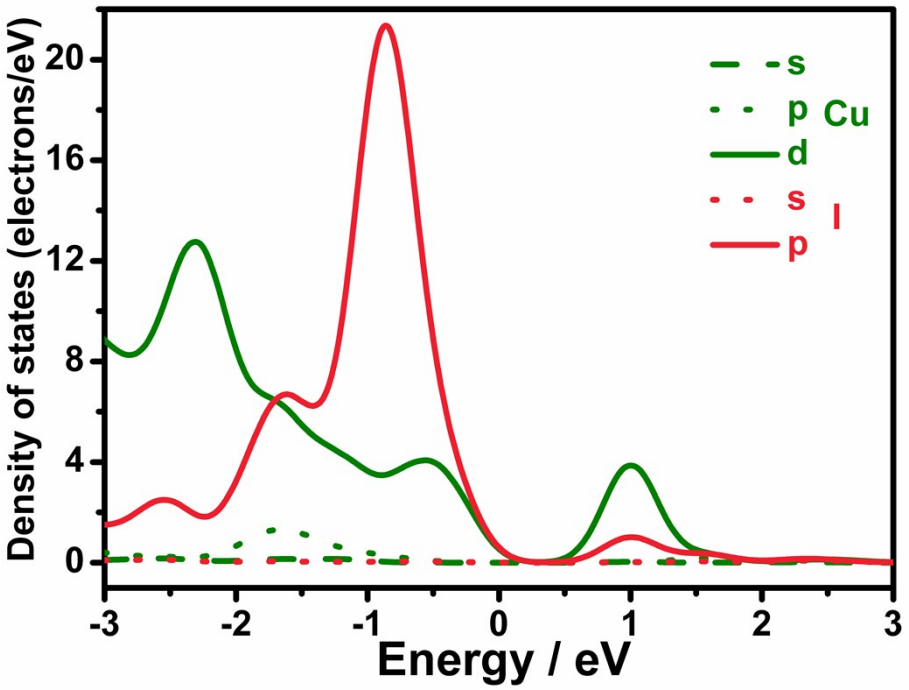

Figure S8. Partial DOS of I and Cu in $[Cu(2,2'\text{-Bipy})_2I]^+$ for **1.**

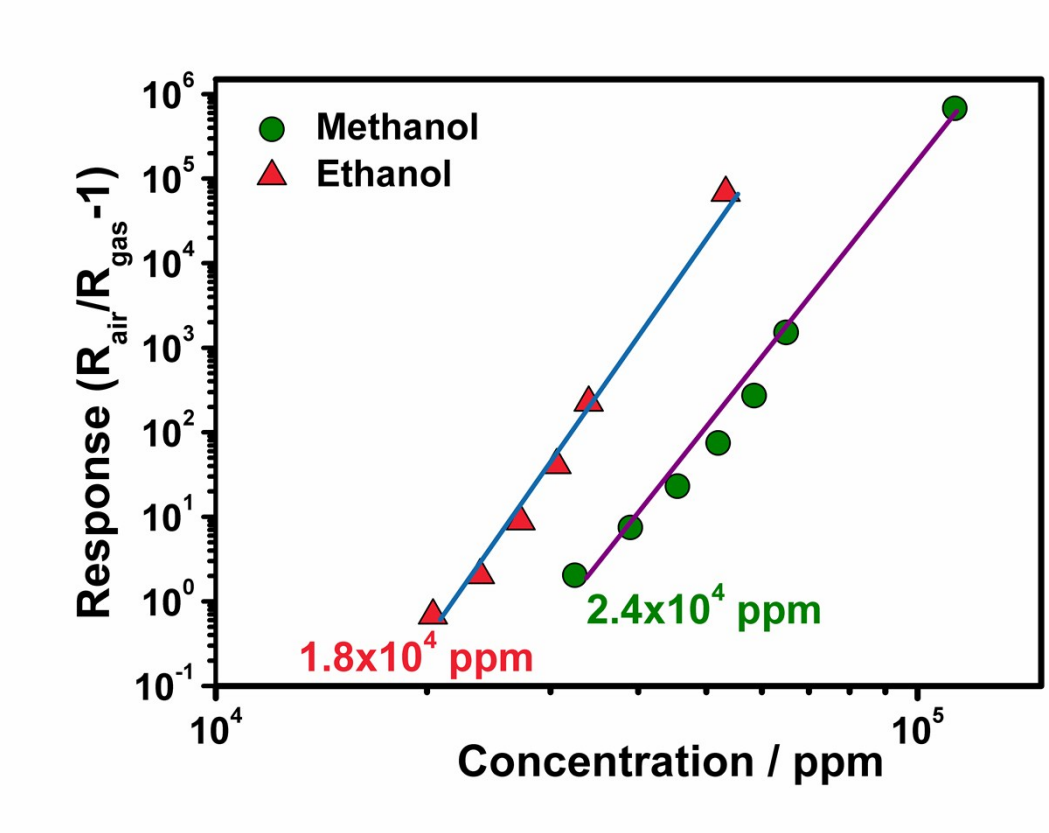

Figure S9. Log-log plots of response (R_{air}/R_{gas} −1) *vs* concentration for methanol and ethanol.

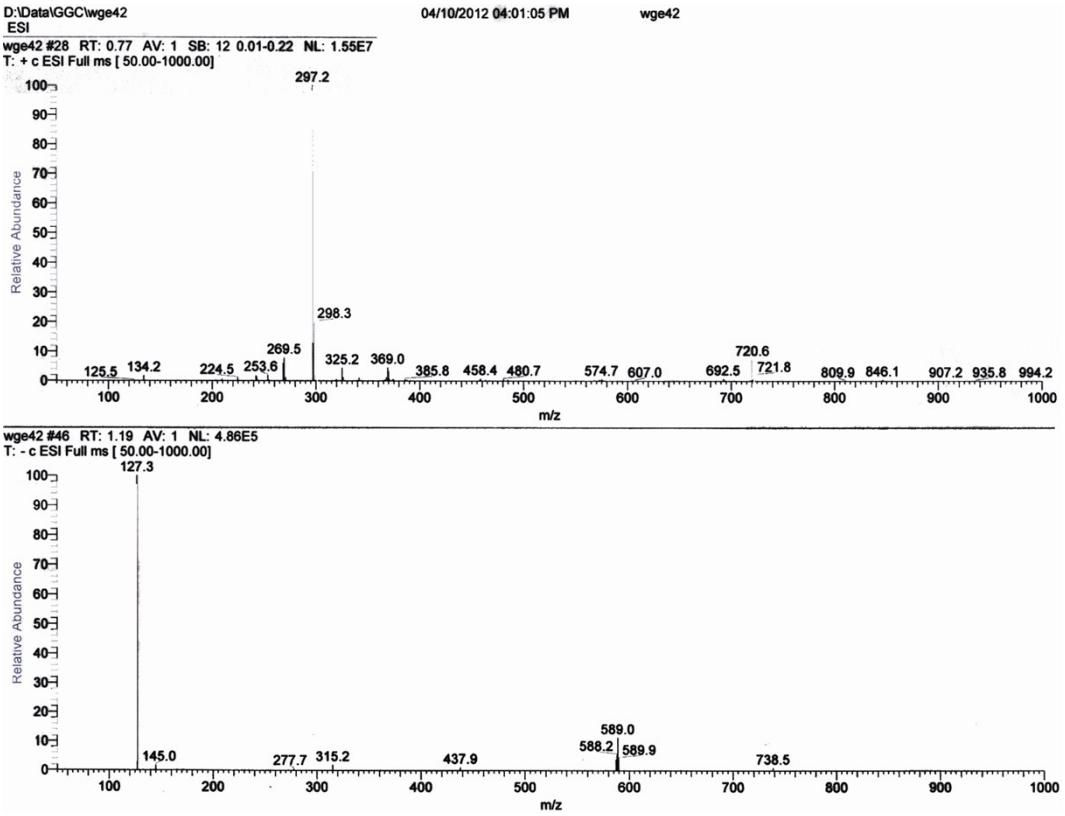

Figure S10. LC-ESI-MS^n spectrum of **2**.

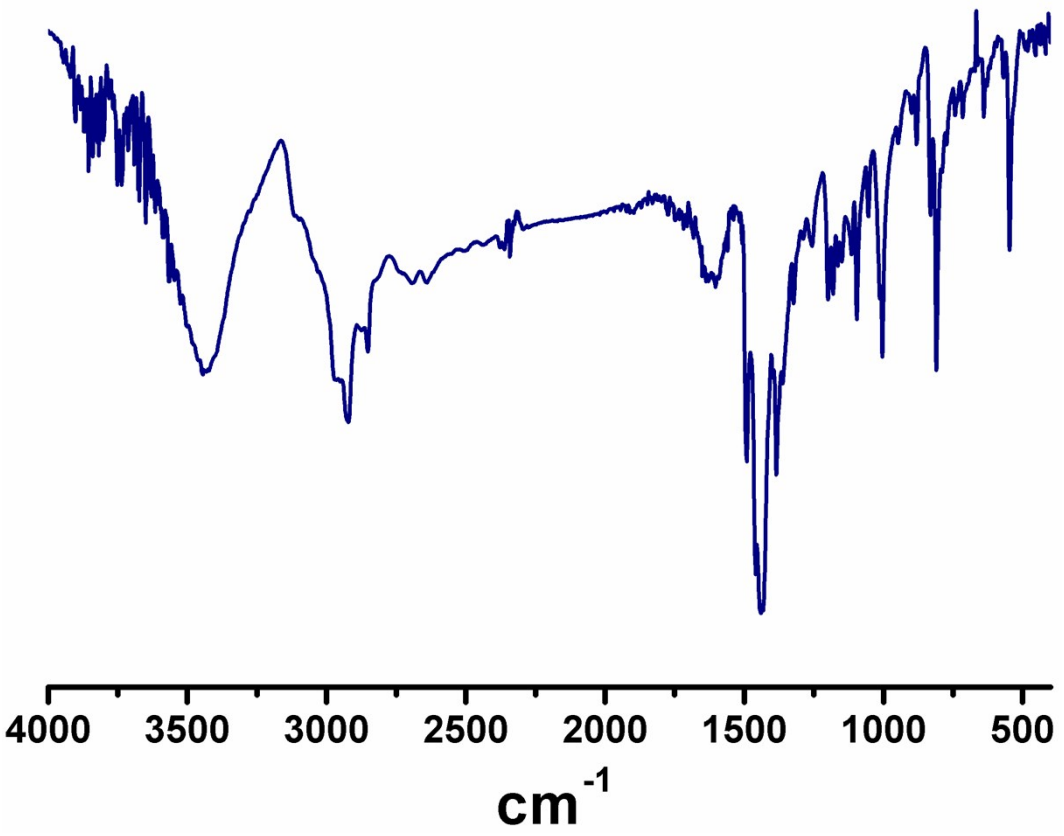

Figure S11. IR spectroscopy of **2**.

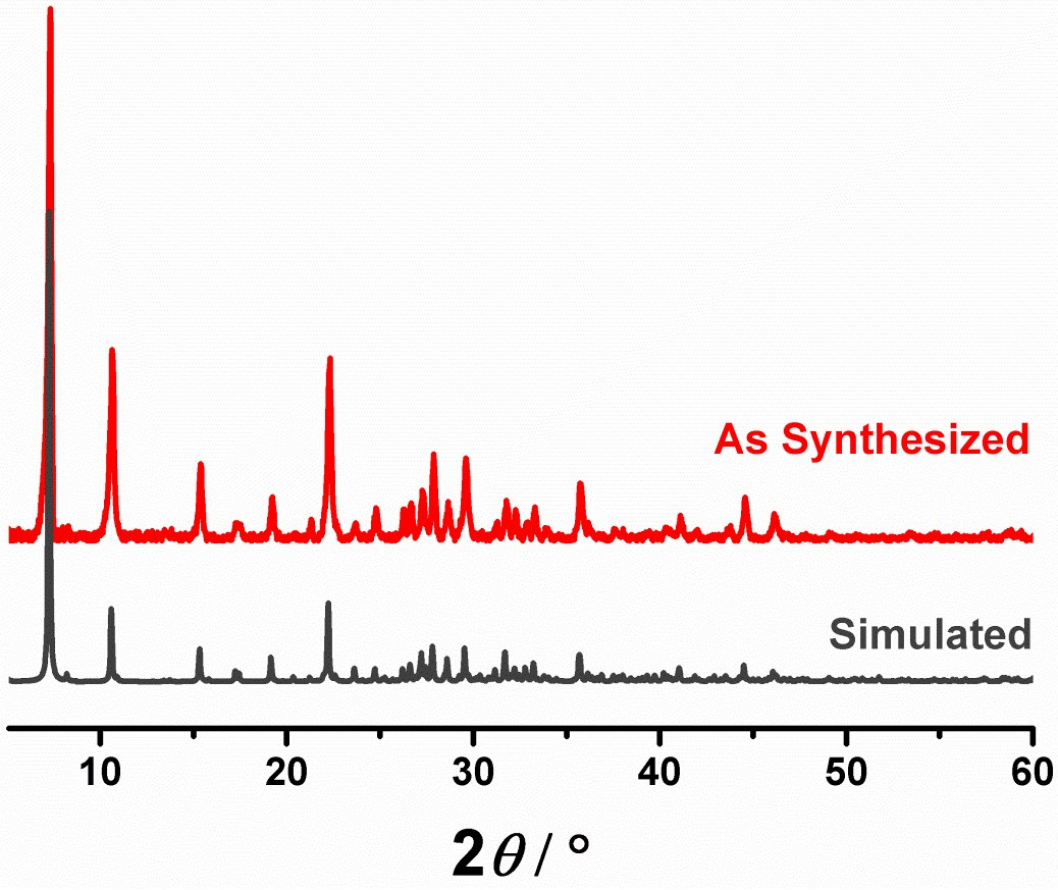

Figure S12. PXRD spectra of the simulated and synthesized sample **2**.

---

[1] M.-S. Yao , W.-X. Tang , G.-E Wang , B. Nath , G. Xu, *Adv. Mater*. **2016**, *28*, 5229–5234.

[2] (a) M. D'Arienzo, L. Armelao, C. M. Mari, S. Polizzi, R. Ruffo, R. Scotti, F. Morazzoni, *J. Am. Chem. Soc.* **2011**, *133,* 5296−5304; (b) R. W. J. Scott, S. M. Yang, G. Chabanis, N. Coombs, D. E. Williams, G. A. Ozin, *Adv. Mater.* **2001**, *13,* 1468−1472; (c) R. W. J. Scott, S. M. Yang, N. Coombs, G. A. Ozin, D. E. Williams, *Adv. Funct. Mater.* **2003**, *13,* 225−231; (d) C. O. Park, S. A. Akbar, *J. Mater. Sci*. **2003**, *38*, 4611−4637.